

# Light Confinement by a Cylindric Metallic Waveguide in Dense Buffer Gas Environment

Ulrich Vogl,\* Anne Saß, Frank Vewinger, and Martin Weitz

*Institut für Angewandte Physik der Universität Bonn,  
Wegelerstr. 8, D-53115 Bonn, Germany*

Alexander Solovev, Yongfeng Mei, and Oliver Schmidt

*Institute for Integrative Nanosciences, IFW Dresden,  
Helmholtzstr. 20, D-01069 Dresden, Germany*

(Dated: January 4, 2012)

## Abstract

We report on the implementation of metallic microtubes in a system of rubidium vapour at 230 bar of argon buffer gas. The high buffer gas pressure leads to a widely pressure broadened linewidth of several nanometers, interpolating between the sharp atomic physics spectra and the band structure of solid state systems. Tube-like metallic waveguide structures have been inserted in the high pressure buffer gas system, allowing for guiding light in an optical dense gas over a length in the tube of up to 1 mm. The system holds promise for nonlinear optics experiments and the study of atom-light polariton condensation.

PACS numbers: 32.80.-t, 05.30.Jp, 32.70.Jz, 42.50.Fx, 42.82.Et, 78.67.Ch

---

\*Electronic address: vogl@iap.uni-bonn.de

Confinement of optical radiation is a key prerequisite in experiments investigating Bose-Einstein condensation of polaritons. It allows to tailor the dispersion relation for this quasiparticles and enhances the obtainable matter-light interaction. Experimentally, exciton-polariton systems in microcavity structures gave evidence of quasiparticle condensation [1–3]. In a recent experiment, thermalization [4], and subsequently Bose-Einstein condensation [5] of a photon gas in a dye-filled optical microcavity has been observed, which emphasizes the capacity of this general approach.

A successful system for light confinement are e.g. hollow core fibers, which in principle allow strong light-matter coupling over long distances in a defined volume with a well defined intensity distribution [6–9]. The enhanced interaction in such systems has proven advantageous for electromagnetically induced transparency and four-wave-mixing [10, 11] with alkali vapour inside the fiber. Most of these experiments require careful procedures to coat the inside of the fiber with certain carbon hydrides to avoid chemical adsorption of the alkali atoms to the silica bulk of the fiber and is thus not applicable for hot vapour, but also successful metal-coating has been shown [12].

In this paper we investigate metal waveguides in a system of hot rubidium vapour at 550 Kelvin and 200 bar of argon buffer gas pressure. The frequent collisions of the rubidium atoms with the buffer gas give a pressure broadened linewidth of a few nanometers, approaching the thermal energy  $k_B T$  of the system in wavelength units. We have shown recently that the frequent collisions with the buffer gas atoms can lead to thermal equilibrium of dressed states, i.e. coupled atom-light states [13, 14]. The nanosecond lifetimes of alkali excited states in high pressure buffer gas ( $\tau_{nat} \simeq 27$  ns for the case of the 5P state of the rubidium atom) is orders of magnitude longer than the picoseconds relaxation times of typical exciton-polariton systems. Thus, there are prospects that atomic physics based polariton condensation experiments can achieve longer coherence times than exciton polariton systems. Another interesting possibility in this system are novel laser cooling schemes [15], which in a thermodynamic sense may also be seen as a consequence of coupling internal and external atomic degrees of freedom in the pressure broadened system. On the other hand, the high required temperatures of the rubidium-high pressure buffer gas system (350°C are required to reach 1 mbar Rb vapour pressure, which is the typical equivalent to an optically dense buffer gas broadened system) make it experimentally challenging to implement the required optical resonator or waveguide structures for a particle-like tailoring of the dispersion

relation in the alkali vapour environment. Standard quartz-based optical fiber structures or mirrors are known to adsorb alkali vapour at temperatures above 150-200°C. Similarly, organic protective coatings become unstable at the used high temperatures. An interesting alternative possibility is the use of metallic microstructures, which have higher chemical stability under the here present conditions. Novel manufacturing techniques have recently allowed for the fabrication of ultra thin, rolled metal tubes that can stand the mentioned preconditions [16]. In this work we report on the implementation of metallic microtubes into a system of rubidium atoms at 230 bar argon buffer gas pressure. The ultra thin microscopic ( $6\mu\text{m}$  diameter) metal structures allow to guide light over a distance of 1 mm in the high pressure buffer gas environment. Albeit the harsh environment the waveguide structures do not show deterioration, even after illuminating with a laser power of 1 Watt.

A drawback of metallic waveguides is their relatively large loss compared to dielectric waveguides, which is due to resistive losses in the metal. Compared to massive metallic structures thin-walled structures with wall thickness of order of the skin-depth can in principle lead to an enhanced transmission [19, 20]. A further notable benefit of such metal structures is that light confinement to diameters below the size of the wavelength can be achieved, an issue that has allowed for extraordinarily high transmission through subwavelength diameter holes [21]. In an interesting experiment with a planar configuration with similar subwavelength silver layers the strong coupling regime could be realized [22]. The silver layers in this experiment formed a low-Q cavity and the strong coupling could be realized with the metal boundary condition providing a stronger confinement than dielectric cavity mirrors.

Let us begin by discussing a few general features of the used metallic microtube structures. Such microstructures can be engineered with high precision by depositing, releasing and rolling up thin metallic membranes [16, 17]. The fabrication process of these tubes allows for a wide variety of diameters from nanometer to several micrometer and a length up to a few millimeter, resulting in aspect ratios of up to 1:10000. The technique is applicable to a variety of materials including combinations of semiconductors, metals and oxides [18]. Figure 1a shows a Scanning Electron Microscopy (SEM) image of a rolled up microtube fabricated on silicon substrates by underetching of photoresist sacrificial layer. The prepared microtube consists of Ni/Fe/Ag layers and has an internal diameter of  $6\pm0.3\mu\text{m}$ . Figure 1b shows a SEM image of a microtube transported onto a metallic holder for the integration into

the optical setup. The inset of Figure 1b indicates sandwiched Ni/Fe/Ag rolled up layers. A general description for the production of these waveguides can be found in [17], for the here used samples we applied the following steps: The Ni/Fe/Ag microtubes were fabricated by electron-beam deposition of metals onto lithographically patterned photoresist layers. Square AR-P 3510 photoresist patterns with the length of 1 mm were prepared on 1.5-inch silicon wafer. Photoresist was spin-coated at 3500 rpm for 35 s, followed by a soft bake using a hotplate at 90°C degrees for 1 minute and exposure to UV light with a Karl Suss MA56 Mask Aligner (410-605 nm). Patterns were developed in a 1:1 AR300-35:H<sub>2</sub>O. Ni/Fe/Ag layers were deposited with corresponding thicknesses 20/20/20 nm on the sample tilted to 65° from the horizontal line. The tubes were then rolled up by underetching of the sacrificial photoresist layer in acetone followed by rinsing in isopropanol. The samples were transferred into the supercritical point dryer to avoid the tube collapsing due to the high capillary pressure (surface tension) of the evaporated solvents. After drying the microtubes were released using glass micro-capillary and transferred on the metallic holder. The fabricated structures are then mounted within the high pressure environment. For the used radiation with wavelength  $\lambda \sim 800$  nm the layer thickness is in the order of the estimated skin depth of the structure (the skin depth of the inner silver layer is approximately 12 nm for the used wavelength and the thickness of the layer [23]).

Our experimental apparatus is shown in Figure 2. A steel chamber with sapphire optical windows is heated to 550 K, yielding 1 mbar rubidium vapour pressure (number density  $10^{16} \text{ cm}^{-3}$ ) and 230 bar argon buffer gas pressure. The metallic waveguide (Figure 1) is placed on a holder inside the cell, facing the entrance window of the cell. Tunable laser radiation from a cw-Titanium-Sapphire laser is directed via a confocal beam geometry to a movable achromatic lens system and then focused into the cell. This setup allows to monitor the location of the laser focus with a control pinhole and simultaneously steer the microtubes to the focal point of the objective. The transmitted light was collected and detected spectrally resolved. In previous experiments [13] we used a freely propagating laser beam, which was tightly focused to a beam waist of  $w_0 = 6 \mu\text{m}$  and directed into the vapour cell. The region of fairly high and uniform intensity is then limited to twice the Rayleigh length  $2z_R = \frac{2\pi w_0^2}{\lambda} = 70 \mu\text{m}$ , with the typical used wavelength of 800 nm. Confinement in a metallic tube over a distance up to 1 mm thus can enhance the effective interaction length by more than an order of magnitude.

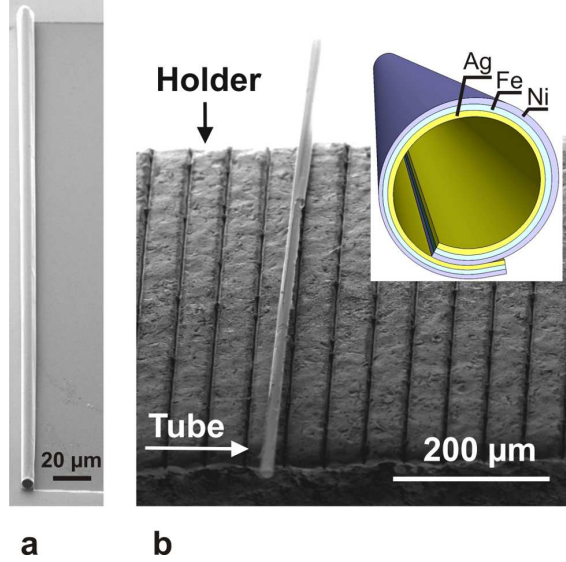


FIG. 1: Single metallic microtube. (a) Scanning electron microscope (SEM) image of a rolled up metallic microtube on silicon substrate. (b) The microtube attached to a metallic holder for the integration into the optical setup.

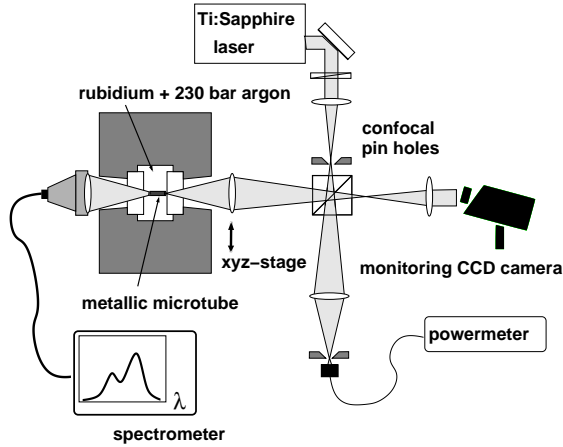


FIG. 2: Experimental setup. With a confocal geometry the position of the laser focus is monitored at a pinhole. A translation stage at the objective allows for lateral scan of the focus position relative to the microtube.

In Fig. 3a we show a typical spectrum in the high pressure buffer gas environment recorded in backwards direction, i.e. unperturbed by transmission effects, where the pressure and saturation broadened rubidium D1 and D2-line resonances are clearly visible. The observed linewidth (FWHM) is roughly 10 nm at the used buffer gas pressure of 230 bar. The spectral width here approaches the thermal energy in the heated gas cell ( $k_B T \approx 20$  nm in wavelength

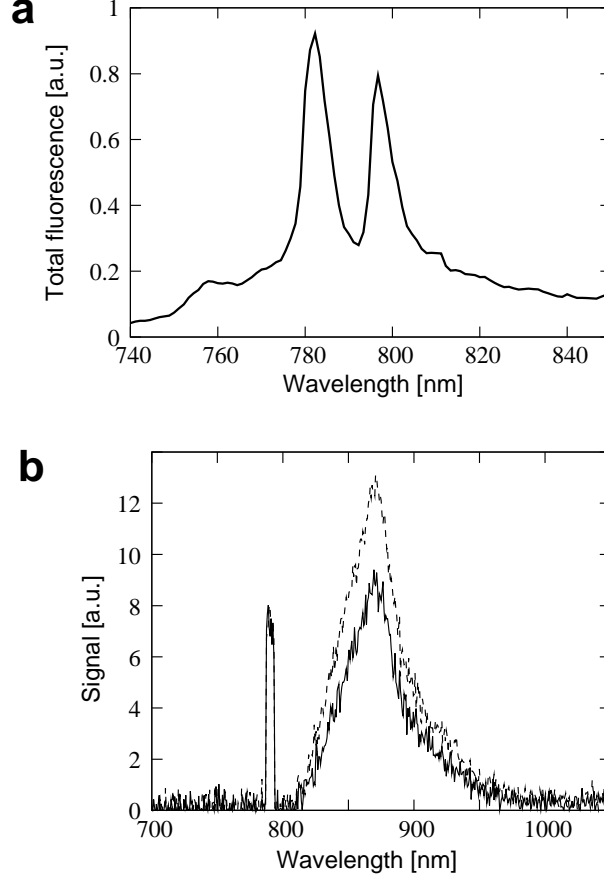


FIG. 3: (a) Spectrum of rubidium with 230 bar argon buffer gas, recorded in backwards direction. The main features are the two fine structure transitions at 780 and 795 nm (Rb D2 and D1 lines respectively). The whole spectrum is strongly pressure broadened. (b) Typical spectra of the radiation detected after the cell versus wavelength for an incident wavelength of 785 nm. One observes a sharp carrier, which is the remainder of the exciting laser, and a broad Stokes-scattered band between 825 and 950 nm. The solid line shows a spectrum for free transmission. An slightly enhanced Stokes-band is observed when the light is coupled into the tube (dashed line).

units at the D-lines wavelengths and 550 K temperature) within an order of magnitude. It is well known that in strongly pressure broadened systems redistribution of the atomic fluorescence can occur [24]. In earlier work we observed that the frequent collisions combined with an excited state lifetime that exceeds the typical collision time by three orders of magnitude leads to a complete redistribution of fluorescence, yielding a spectrum centered around the two fine structure lines at 780 nm and 795 nm in this system [15].

To investigate the possible influence of the microtubes we analyzed the light in forward

direction. A typical corresponding spectrum of the transmitted light after the cell without metal tube is shown by the solid line in Fig. 3b. The used laser wavelength here was near 785 nm, i.e. in the vicinity of the rubidium D-lines, and the visible sharp peak in the spectrum at the incident wavelength is due to remaining transmitted radiation at the carrier wavelength. The used optical density is about 3 at resonance, and most of the fluorescence is multiple reabsorbed and scattered spatially into the full solid angle and spectrally to the far wings of the fluorescence spectrum. A main feature of the measured spectra is a relatively strong and spectrally broad band between 825 and 950 nm.

Scattered radiation that is closer to resonance within the observed spectrum is suppressed, as can be understood by the stronger absorption for near-resonant light, leading to the observed radiation at the end of the cell (apart from a remaining part of the incident laser frequency peak) mainly being far red-shifted radiation. We attribute the observed red-shifted spectral components in Fig. 3b to be mainly due to emission from Rubidium-Argon excimer states [25], comparable to similar features in Rb-He exciplexes [26, 27]. Its origin are optical collisions with large energy exchange, that result in a spectral shift of the fluorescence photons into the transparent region of the vapour. As the end of the metal tube is otherwise poorly accessible within the cell, we use this red shifted spectral band as an indicator for the influence of the metal tube.

To place the microtubes controlled into the optical path we initially matched the position of the tube ending and the focus of the laser beam with the confocal setup shown in Fig. 2 and collected the transmitted light. By a lateral scan of the laser beam in horizontal and vertical direction over the end face of the metal tube we could clearly identify the tube walls by the variation in the transmitted light. In Figure 4 we show the dependence of the spectral part at the carrier wavelength (dashed line) and the part in the Stokes-band between 825-950 nm (solid line) for a horizontal (panel a) and vertical scan (panel b) over the waveguide aperture. The shown data were recorded for an incident wavelength of 775 nm, where both the transmitted carrier and the Stokes band have comparable intensity. Clearly visible is the signature of the tube walls at a distance of circa  $6\text{ }\mu\text{m}$  in both the carrier and the Stokes band signal. The observed attenuation of the total light intensity is small (except for the vertical scan, where the beam hits the tube holder on one side). This alignment and subsequent measurements were performed with a laser power up to 1 W. By monitoring the metal tube no degradation was observed despite the relatively high light intensity at the tube entrance

of  $10^7 \text{ W/cm}^2$ . This shows that the immersion of the metal tube in the dense argon gas provides sufficient heat conduction to prevent melting of the thinwalled structures. When observing the Stokes band, a slight enhancement is visible when the light is coupled into the tube, as can be seen in Fig. 3b. A straightforward explanation for the variation in the Stokes signal is heating of the waveguide by the pumping laser, leading to local changes in the density of Argon and Rubidium. Nevertheless, the overall shape of the spectrum shows that the waveguide does not disturb the Rubidium-Argon system strongly, making it thus a promising candidate for experiments on polariton condensation.

The here investigated cylindrical metal waveguides could be used to confine light to a small volume to achieve atom-light polariton condensation with the waveguide modifying the dispersion relation of the quasiparticles, and possibly also acting as a trapping potential. The combined system of thin-walled metallic waveguides with rubidium vapour in a high buffer gas environment exhibits several qualities that make it a promising candidate for further investigations. The frequent collisions of rubidium atoms with noble gas atoms under optical radiation can drive coupled atom-light states towards thermal equilibrium. This can be further supported by the enhanced interaction within the waveguide. For the future, the waveguides which have now been designed cylindrical with relatively large diameter can be tailored to smaller diameters, which increases the confinement. In particular, for a diameter of order of  $\lambda/2$ , the cut-off wavelength will reach within the redistributed fluorescence spectrum, similarly as in [4]. In this regime we expect that photons - or, when the strong coupling regime is reached, atom light polaritons - thermalize above the cavity cut-off, i.e. their frequencies will be distributed by an amount  $k_B/T$  above the cut-off frequency. The strong transverse confinement makes the system effectively one-dimensional. Furthermore, by using a biconical design as indicated in Fig. 5 a trapping potential can be realized, that in first order is of the form  $V(z) \propto |z|$ , where  $z$  is the direction along the symmetric axis (in analogy to [4]). This linearly confined, one-dimensional system is expected to support a BEC in the ideal gas case at sufficiently low temperatures and high densities (the general requirement is that the trapping potential here should be more confining than parabolic [29]). A detection of the optical radiation could be realized e.g. by collection of the light leaking out through one of the apertures, or for a tube with ultrathin walls by light leaking at the waist of the waveguide.

To conclude, we have shown that metallic microtubes can be integrated in a high pressure



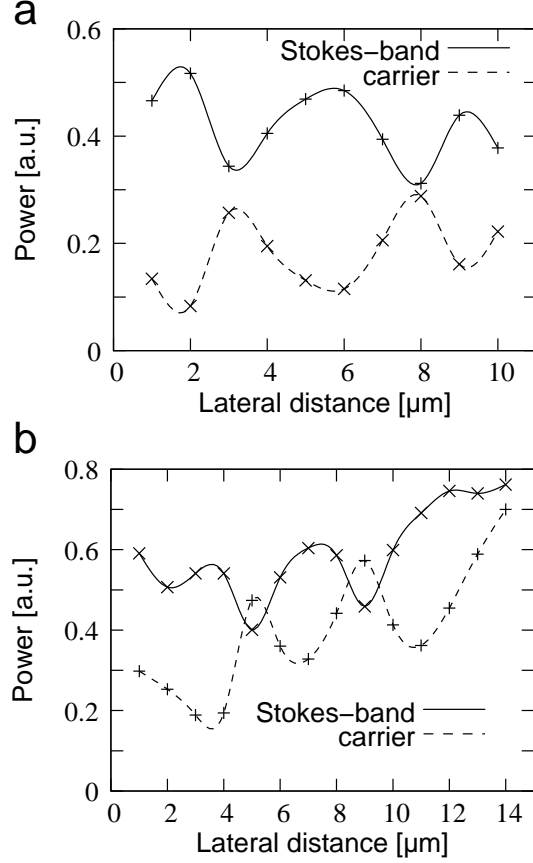


FIG. 4: We performed a transverse scan of the laser beam over the tube entrance both in horizontal (a) and vertical (b) direction (shown are datasets for an incident wavelength of 775 nm). The emitted light was collected and spectrally analyzed. Shown are separately the spectral part of the remaining carrier wavelength (dashed line) and the Stokes-band between 825-950 nm for both cases. We can clearly identify two local drops in the Stokes-band power at a distance of the tube diameter. The drop of the Stokes power is accompanied by a peak in the transmitted carrier power. (The asymmetry in the vertical scan is attributed to the tube mounting).

buffer gas optical spectroscopy setup. The material properties allow investigations in experimental regimes that are not easily accessible with comparable structures based on silica. Due to the high thermal conductivity of the metal and the surrounding argon gas, light intensities of up to  $10^7 \text{ W/cm}^2$  have been applied without thermal degradation. These highly versatile structures could pave the way to new approaches in the strong coupling between light and matter, or more specific for the investigation of collective atom-light states. Further investigations will include the study of smaller structures and waveguides with broken

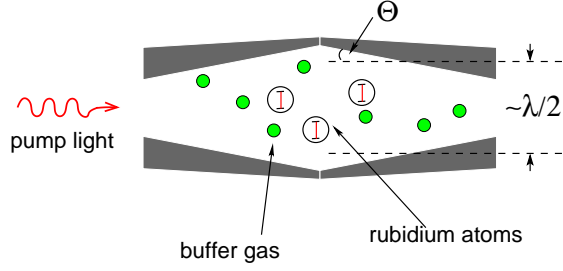


FIG. 5: Proposed biconical waveguide design with cut-off within the redistributed fluorescence spectrum of rubidium. The system can be optically pumped with short-wavelength light exciting the pressure broadened rubidium resonances. Subsequent redistribution of fluorescence towards longer wavelength can accumulate photons near the cut-off of the waveguide. The diameter of the structure should be in the order of  $\lambda/2$  of the used laser wavelength. A nonvanishing inner cone angle  $\Theta$  of the biconical structure allows for the tailoring of the allowed modes inside the cavity [28], and provides a trapping potential along the weakly confined axis.

axial symmetry.

Financial support from the DFG within the focused research unit FOR557 and under the cooperation project 436RUS113/996/0-1 is acknowledged. The authors acknowledge helpful discussions with A. P. Alodjants and I. Y. Chestnov.

- 
- [1] J. Kasprzak, M. Richard, S. Kundermann, A. Baas, P. Jeambrun, J. M. J. Keeling, F. M. Marchetti, M. H. Szymanska, R. Andre, J. L. Staehli, V. Savona, P. B. Littlewood, B. Deveaud and L. S. Dang. *Bose-Einstein condensation of exciton polaritons*. Nature **443**, 409 (2006).
  - [2] C. W. Lai, N. Y. Kim, S. Utsunomiya, G. Roumpos, H. Deng, M. D. Fraser, T. Byrnes, P. Recher, N. Kumada, T. Fujisawa and Y. Yamamoto. *Coherent zero-state and  $\pi$ -state in an exciton-polariton condensate array*. Nature (London) **450**, 529 (2007).
  - [3] A. Amo, J. Lefrère, S. Pigeon, C. Adrados, C. Ciuti, I. Carusotto, R. Houdré, E. Giacobino and A. Bramati. *Superfluidity of polaritons in semiconductor microcavities*. Nature Physics **5**, 805 (2009).
  - [4] J. Klaers, F. Vewinger and M. Weitz. *Thermalisation of a two-dimensional photonic gas in a white-wall photon box*. Nature Physics **6**, 512 (2010).

- [5] J. Klaers, J. Schmitt, F. Vewinger and M. Weitz. *Bose-Einstein condensation of photons in an optical microcavity*. Nature **468**, 545 (2010).
- [6] R. F. Cregan, B. J. Mangan, J. C. Knight, T. A. Birks, P. S. J. Russell, P. J. Roberts and D. C. Allan. *Single-Mode Photonic Band Gap Guidance of Light in Air*. Science **285**, 1537 (1999).
- [7] S. Ghosh, J. E. Sharping, D. G. Ouzounov and A. L. Gaeta. *Resonant Optical Interactions with Molecules Confined in Photonic Band-Gap Fibers*. Physical Review Letters **94**, 093902 (2005).
- [8] M.-L. Hu, C.-Y. Wang, Y.-J. Song, Y.-F. Li, L. Chai, E. E. Serebryannikov and A. M. Zheltikov. *A hollow beam from a holey fiber*. Optics Express **14**, 4128 (2006).
- [9] M. Bajcsy, S. Hofferberth, V. Balic, T. Peyronel, M. Hafezi, A. S. Zibrov, V. Vuletic and M. D. Lukin. *Efficient All-Optical Switching Using Slow Light within a Hollow Fiber*. Physical Review Letters **102**, 203902 (2009).
- [10] F. Benabid, F. Couny, J. C. Knight, T. A. Birks and P. S. J. Russell. *Compact, stable and efficient all-fibre gas cells using hollow-core photonic crystal fibres*. Nature (London) **434**, 488 (2005).
- [11] P. Londero, V. Venkataraman, A. R. Bhagwat, A. D. Slepko and A. L. Gaeta. *Ultralow-Power Four-Wave Mixing with Rb in a Hollow-Core Photonic Band-Gap Fiber*. Physical Review Letters **103**, 043602 (2009).
- [12] F. K. Fatemi, M. Bashkansky, E. Oh and D. Park. *Efficient excitation of the TE<sub>01</sub> hollow metal waveguide mode for atom guiding*. Opt. Express **18**, 323 (2010).
- [13] U. Vogl and M. Weitz. *Spectroscopy of atomic rubidium at 500-bar buffer gas pressure: Approaching the thermal equilibrium of dressed atom-light states*. Phys. Rev. A **78**, 011401 (2008).
- [14] I. Y. Chestnov, A. P. Alodjants, S. M. Arakelian, J. Nipper, U. Vogl, F. Vewinger and M. Weitz. *Thermalization of coupled atom-light states in the presence of optical collisions*. Phys. Rev. A **81**, 053843 (2010).
- [15] U. Vogl and M. Weitz. *Laser Cooling by Collisional Redistribution of Radiation*. Nature, London **461**, 70 (2009).
- [16] A. Solovev, Y. Mei, E. Bermúdez Ureña, G. Huang and O. G. Schmidt. *Catalytic Microtubular Jet Engines Self-Propelled by Accumulated Gas Bubbles*. Small **5**, 1688 (2009).

- [17] Y. Mei, G. Huang, A. A. Solovey, E. Bermúdez Ureña, I. Mönch, F. Ding, T. Reindl, R. K. Y. Fu, P. K. Chu and O. G. Schmidt. *Versatile Approach for Integrative and Functionalized Tubes by Strain Engineering of Nanomembranes on Polymers*. Advanced Materials **20**, 4085 (2008).
- [18] O. G. Schmidt and K. Eberl. *Nanotechnology: Thin solid films roll up into nanotubes*. Nature (London) **410**, 168 (2001).
- [19] J. Takahara, S. Yamagishi, H. Taki, A. Morimoto and T. Kobayashi. *Guiding of a one-dimensional optical beam with nanometer diameter*. Optics Letters **22**, 475 (1997).
- [20] H. F. Ghaemi, T. Thio, D. E. Grupp, T. W. Ebbesen and H. J. Lezec. *Surface plasmons enhance optical transmission through subwavelength holes*. Phys. Rev. B **58**, 6779 (1998).
- [21] J. Rybczynski, K. Kempa, A. Herczynski, Y. Wang, M. J. Naughton, Z. F. Ren, Z. P. Huang, D. Cai and M. Giersig. *Subwavelength waveguide for visible light*. Applied Physics Letters **90**, 021104 (2007).
- [22] P. A. Hobson, W. L. Barnes, D. G. Lidzey, G. A. Gehring, D. M. Whittaker, M. S. Skolnick and S. Walker. *Strong exciton-photon coupling in a low-Q all-metal mirror microcavity*. Applied Physics Letters **81**, 3519 (2002).
- [23] Z. Wang, X. Cai, Q. Chen and L. Li. *Optical properties of metal-dielectric multilayers in the near UV region*. Vacuum **80**, 438 (2006).
- [24] C. Cohen-Tannoudji, J. Dupont-Roc and G. Grynberg. *Atom-Photon Interactions - Basic Processes and Applications* (Wiley, New York, 1992).
- [25] J. Pascale and J. Vandeplanque. *Excited molecular terms of the alkali-rare gas atom pairs*. J. Chem. Phys. **60**, 2278 (1974).
- [26] K. Hirano, K. Enomoto, M. Kumakura, Y. Takahashi and T. Yabuzaki. *Emission spectra of  $Rb^*He_n$  exciplexes in a cold  $^4He$  gas*. Phys. Rev. A **68**, 012722 (2003).
- [27] J. F. Sell, M. A. Gearba, B. M. Patterson, T. Genda, B. Naumann and R. J. Knize. *Enhancement of Rb fine-structure transfer in  $^4He$  due to three-body collisions*. Opt. Lett. **35**, 2146 (2010).
- [28] V. Kravchenko, V. Veretel'nik and V. L. Rvachev. *Calculation of electrodynamic properties of a biconical resonator*. Measurement Techniques **36**, 337 (1993).
- [29] V. Bagnato and D. Kleppner. *Bose-Einstein condensation in low-dimensional traps*. Phys. Rev. A **44**, 7439 (1991).